

Molecular beam epitaxy growth and characterization of broken-gap (type II) superlattices and quantum wells for midwave-infrared laser diodes

T. C. Hasenberg^{a)}

Department of Physics and Astronomy, 144 IATL, University of Iowa, Iowa City, Iowa 52242

P. S. Day

Department of Electrical and Computer Engineering, 144 IATL, University of Iowa, Iowa City, Iowa 52240

E. M. Shaw, D. J. Magarrell, J. T. Olesberg, C. Yu, Thomas F. Boggess,^{b)}
and M. E. Flátte

Department of Physics and Astronomy, 144 IATL, University of Iowa, Iowa City, Iowa 52242

(Received 10 October 1999; accepted 15 February 2000)

We have developed a broken-gap (type II) quantum well active region for midwave infrared interband lasers which exhibits a significantly increased Auger lifetime over that of previous designs. © 2000 American Vacuum Society. [S0734-211X(00)09003-X]

I. INTRODUCTION

Midwave infrared (MWIR) lasers have important applications including trace gas sensing and military countermeasures, as well as medical applications such as noninvasive glucose monitoring. Room temperature operation of MWIR interband lasers has been difficult because of the presence of significant Auger recombination (AR) and intersubband absorption (ISBA). Auger recombination occurs when a carrier pair recombines and transfers energy and momentum to another carrier. ISBA involves an optically induced transition between either valence or conduction subbands. It is detrimental to a laser when it occurs at the lasing wavelength due to the presence of an energy subband positioned approximately one lasing transition energy from either the conduction or valence band edge. These undesirable effects can be suppressed by using strain and quantum confinement to tailor the energy bands in order to reduce the number of electron (hole) states which are one lasing transition energy away from the conduction (valence) band and/or by balancing the conduction and valence band density of states.¹

The initial type-II MWIR laser development work employed multiple quantum well (MQW) samples with InAs/GaInSb broken-gap superlattice (BGSL) wells.^{2,3} The BGSL approach to MWIR lasers allows an extra degree of freedom as compared to the more conventional approach of employing InGaAsSb quaternary active regions. One can independently vary the thicknesses of the two constituent layers as well as the composition of the GaInSb compound. This allows one to independently tune the band structure and the effective lattice constant of the structure. Numerous laser diodes were demonstrated in the 2.8–4.3 μm wavelength range, however, the suppression of AR and ISBA was somewhat limited with the two-layer BGSL structure.⁴ Therefore the InAs/GaInSb/InAs/InGaAlAsSb four-layer BGSL was developed. Although significant reductions in AR and ISBA were obtained,⁵ poor hole transport was observed in these

structures.⁶ Hence, a laser active region composed of InAs/AlAsSb/InAs/GaInSb/InAs/AlAsSb/InAs broken-gap quantum wells (BGQW) has been proposed in order to obtain both high optical gain and good carrier transport. BGQW samples have been grown by molecular beam epitaxy (MBE) and have exhibited improved suppression of AR and ISBA when compared to the previous BGSL designs. The MBE parameters and shutter sequences employed during the growth of these samples, as well as the observed carrier lifetimes are presented.

The first MWIR lasers with (type-II misaligned) broken-gap active regions employed MQW structures with two-layer InAs/Ga_{0.75}In_{0.25}Sb BGSL wells and InGaAsSb barriers.³ MQW structures were necessary because the two-layer BGSL wells have a high degree of compressive strain. The InGaAsSb barriers were grown with tensile strain to yield a strain balanced well/barrier combination. However, these structures had relatively high AR and ISBA rates due to the large density of hole states one band gap below the HH1 level and due to the poor balancing of the conduction and valence band edge density of states (DOS).¹

A Perkin Elmer 430P MBE machine equipped with solid-source group III effusion cells was used for sample growth. The arsenic cell was an EPI model VC-III valved cracker unit which allowed rapid changes in the arsenic dimer flux. The EPI model 175 antimony cell emitted a predominantly monomer flux as a result of the 925 °C cracking zone temperature that was utilized.

MQW samples employing ten 225 Å thick Ga_{0.75}In_{0.25}Sb/InAs BGSL wells separated by nine 400 Å thick In_{0.20}Ga_{0.60}Al_{0.20}As_{0.17}Sb_{0.83} barrier layers [Fig. 1(a)] were grown at 380 °C for direct measurement of the carrier lifetimes. The MQW was bracketed on both ends by 1000 Å thick In_{0.20}Ga_{0.60}Al_{0.20}As_{0.17}Sb_{0.83} cladding layers. The quantum wells consist of 4.5 period Ga_{0.75}In_{0.25}Sb(36 Å)/InAs(15 Å) broken-gap superlattices (i.e., starting and ending with GaInSb). Five-second antimony soaks were utilized after the InAs and GaInSb layers in order to obtain InSb-like interfaces between these layers. This procedure has been shown to yield more abrupt interfaces with stronger room

^{a)}Electronic mail: thomas-hasenberg@uiowa.edu

^{b)}Also at: Dept of Electrical and Computer Engineering, University of Iowa, Iowa City, Iowa.

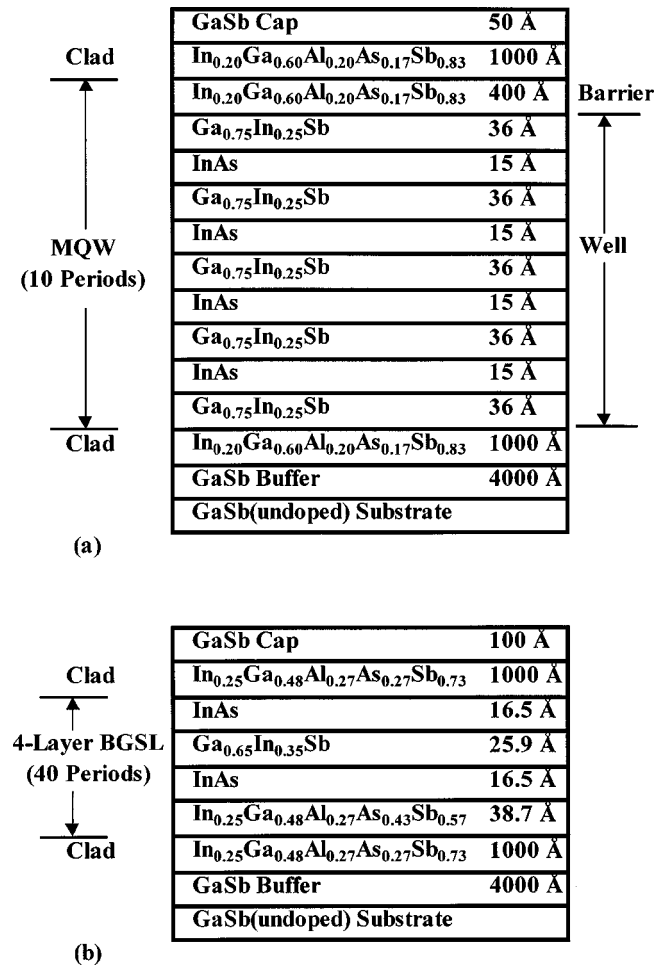


FIG. 1. (a) Schematic of the two-layer GaInSb/InAs broken-gap superlattice (BGSL) MQW structure with InGaAlAsSb barriers. This sample is designed for 3.55 μm laser operation. (b) Schematic of the four-layer BGSL structure. The utilization of the InGaAlAsSb strain-balancing layer in the BGSL allows one to use a more highly strained GaInSb layer than in the two-layer structure.

temperature photoluminescence than GaAs-like interfaces.⁷ Finally, a 50 Å GaSb cap layer was grown on top of the upper In_{0.20}Ga_{0.60}Al_{0.20}As_{0.17}Sb_{0.83} cladding layer, and the sample was annealed at 500 °C for 30 min in an antimony flux. The anneal was found to significantly improve the 300 K optical efficiencies in the samples presumably by reducing the densities and/or optical activities of native defects.⁸

Ultrafast pump/probe measurements were performed on these samples utilizing a 830 nm Ti:sapphire pump beam and a MWIR probe beam generated with an optical parametric oscillator. By measuring the room temperature differential transmission as a function of probe delay time and repeating at multiple fluences, the Auger lifetimes and Shockley Read Hall (SRH) lifetimes were determined.² A two-layer BGSL sample designed for 3.55 μm laser emission [Fig. 1(a)] yielded a 4.2 ns SRH lifetime and a 130 ps Auger lifetime at a carrier concentration calculated to be appropriate for lasing ($n = 7.8 \times 10^{17} \text{ cm}^{-3}$).

Several laser diodes spanning the 2.8–4.3 μm range were demonstrated using similar two-layer BGSLs as active re-

gions. These include an eight-period MQW device with Ga_{0.75}In_{0.25}Sb(39 Å)/InAs(12.5 Å) BGSL wells and In_{0.25}Ga_{0.75}As_{0.22}Sb_{0.78} barriers. This device operated pulsed up to 255 K at a 3.2 μm wavelength and operated continuous wave (CW) up to 180 K.⁴

In an attempt to further reduce AR and ISBA, a new BGSL was designed by adding a strain balancing quinary layer and a second InAs layer to the two-layer structure. This design resulted in a four-layer InAs/Ga_{0.65}In_{0.35}Sb/InAs/In_{0.25}Ga_{0.48}Al_{0.27}As_{0.43}Sb_{0.57} strain-balanced BGSL structure. The utilization of the In_{0.25}Ga_{0.48}Al_{0.27}As_{0.43}Sb_{0.57} quinary layer allows the use of a more heavily strained GaInSb layer and allows one to grow thick (i.e., many period) BGSL structures. Hence, the need for strain-balancing barrier layers as utilized in the two-layer BGSL samples is eliminated.

Samples designed for 3.5 μm laser emission employing thick (40 period) InAs(16.5 Å)/Ga_{0.65}In_{0.35}Sb(25.9 Å)/InAs(16.5 Å)/In_{0.25}Ga_{0.48}Al_{0.27}As_{0.43}Sb_{0.57}(38.7 Å) four-layer BGSLs were grown on GaSb substrates with 1000 Å thick In_{0.25}Ga_{0.48}Al_{0.27}As_{0.27}Sb_{0.73} cladding layers [Fig. 1(b)]. The four-layer sample was grown at 380 °C and, like the two-layer design, employed five-second antimony soaks after all of the InAs, GaInSb, and InGaAlAsSb layers in the BGSL. After growth, the sample was annealed at 500 °C for 30 min in an antimony flux.

Four-layer BGSL samples with excellent structural quality have been grown as exhibited by x-ray diffraction measurements (Fig. 2). The sharpness and intensity of the superlattice fringes observed in the spectrum indicate the presence of abrupt interfaces. Good agreement is obtained between the observed spectrum and the one calculated for this structure using a dynamical x-ray model. The measured superlattice fringe spacing indicates an 89.4 Å BGSL period. An additional indication of sample quality was exhibited by the presence of strong room temperature photoluminescence (PL) which was peaked at 3.84 μm . The layer thicknesses and alloy compositions of the structure were determined using a self-consistent analysis of the x-ray diffraction spectrum, the PL spectrum and the MBE fluxes and shutter times.⁹

These optimized four-layer BGSL samples [Fig. 1(b)] were designed using a $\mathbf{K}\cdot\mathbf{p}$ band structure formalism. AR was minimized by reducing the valence band edge density of states. This is accomplished by introducing strain into the active region. ISBA was optimized by decreasing the number of states within one lasing transition of the band edges. The theoretical predictions of reduced Auger recombination were experimentally verified by pump/probe measurements (Fig. 3). The aforementioned four-layer BGSL sample exhibited an Auger lifetime of 350 ps at the calculated optimal carrier density ($n = 9.5 \times 10^{17} \text{ cm}^{-3}$) for lasing at 300 K (upper arrow in Fig. 3).⁶ To further test the design, double heterostructure 2.7, 3.7, and 5.2 μm wavelength diode lasers were fabricated using thick four-layer BGSL active regions. Unfortunately, only the 2.7 μm devices lased under electrical injection. Poor vertical hole transport through the thick four-layer BGSLs and nonuniform carrier distribution limited di-

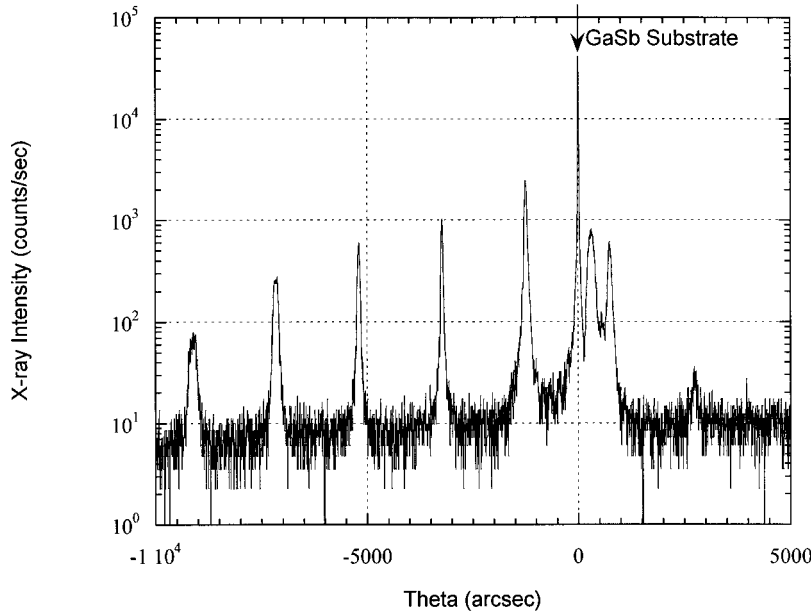


FIG. 2. X-ray spectrum for a four-layer BGSL sample. The spacing of the superlattice fringes is consistent with an 89.4 Å BGSL period. The sharp, intense peaks are indicative of abrupt interfaces in the BGSL.

ode device performance. Nevertheless, the 3.7 and 5.2 μm devices lased up to 300 and 185 K, respectively, with optical pumping.¹⁰

Most recently, we have designed, grown, and characterized an InAs/AlAs_{0.15}Sb_{0.85}/InAs/Ga_{0.60}In_{0.40}Sb/InAs/AlAs_{0.15}Sb_{0.85}/InAs BGQW structure (Fig. 4) that is predicted to have electronic and optical properties superior to that of the four-layer BGSL. The thicknesses of the InAs, AlAsSb, and GaInSb layers are 14, 21, and 25 Å, respectively. In this structure the hole transport problem present in the four-layer samples is substantially reduced by removing the (hole barrier) quaternary layer, yet suppression of AR and ISBA is improved. This structure was grown under slightly different conditions than the previous two. The optimum growth temperature for the quantum well active region was found to be slightly hotter (410 °C) than for the previous

BGSL samples, presumably due to the presence of the AlAsSb layers. Again, five-second antimony soaks were employed after the InAs, AlAs_{0.15}Sb_{0.85}, and Ga_{0.60}In_{0.40}Sb layers and a 30 min, 500 °C postgrowth anneal was employed. In an attempt to maintain good control of the composition, the AlAs_{0.15}Sb_{0.85} layers were grown with the modulated shutter¹¹ technique, with two-second soaks between the AlSb and AlAs portions of the layer. Essentially, the layer was grown as an AlSb/AlAs superlattice since the arsenic and antimony shutters were not open simultaneously. The shutter

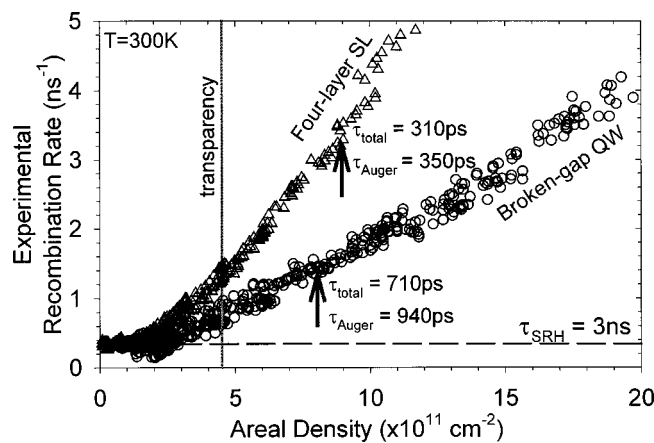


FIG. 3. Plot of the carrier recombination rate as a function of the areal carrier density as determined by ultrafast pump/probe measurements in four-layer BGSL structures and in BGQW samples. The vertical arrow on each curve indicates the calculated optimum carrier density for 300 K laser operation of that structure.

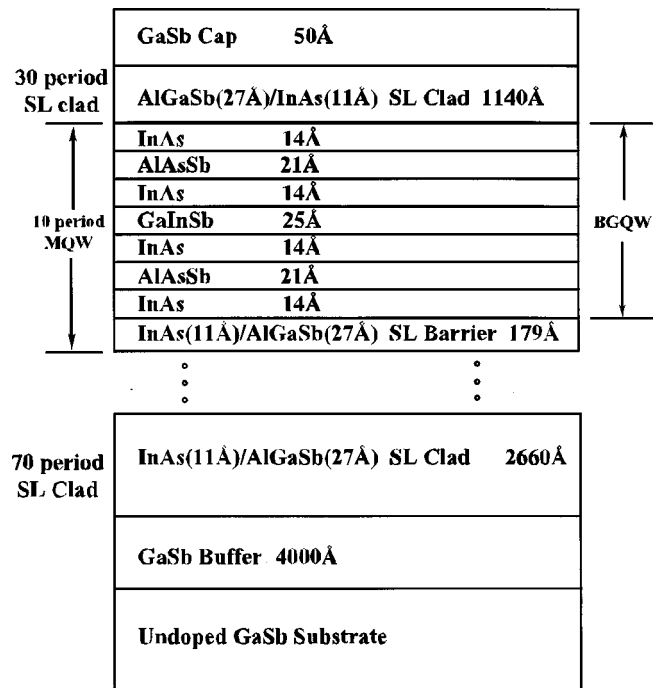


FIG. 4. Schematic drawing of the MQW structure with InAs/AlAsSb/GaInSb broken-gap quantum wells (BGQWs) and InAs/AlGaSb superlattice barriers.

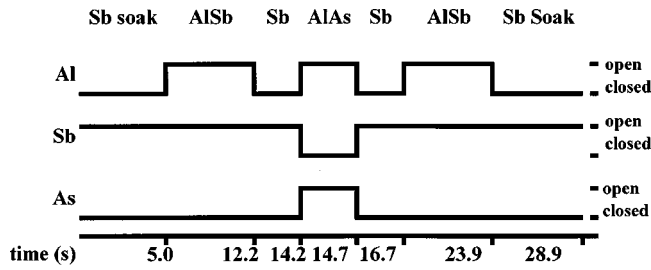


Fig. 5. Shutter sequence for an AlAsSb ternary-like layer grown with the modulated shutter technique.

sequence for this AlAsSb ternary-like layer is shown in Fig. 5. The composition of this layer is critical to the success of the BGQW as a laser active region since it is utilized to strain balance the BGQW structure. If the $\text{AlAs}_{0.15}\text{Sb}_{0.85}$ composition is not accurately controlled, the BGQW will relax and misfit dislocations will form. This will result in short SRH lifetimes and, thereby, poor radiative efficiencies.

$\text{InAs}(11 \text{ \AA})/\text{Al}_{0.60}\text{Ga}_{0.40}\text{Sb}(27 \text{ \AA})$ superlattices (SLs) were utilized as barriers between the BGQWs. These SL barriers were employed because they could be grown with better surface morphologies than the InGaAlAsSb layers used in the previous structures. In addition, the SL gives rise to minibands in contrast to the discrete energy levels of the InGaAlAsSb compound. The minibands allow more efficient injection of electrons and holes from the *n*-type and *p*-type cladding layers, respectively, into the SL barriers.¹² The growth conditions for the barriers were similar to those of the BGQWs with a 410 °C substrate temperature and with five-second antimony soaks after the InAs and AlGaSb layers. As with the four-layer BGSL samples, excellent structural quality and interface abruptness is exhibited by sharp

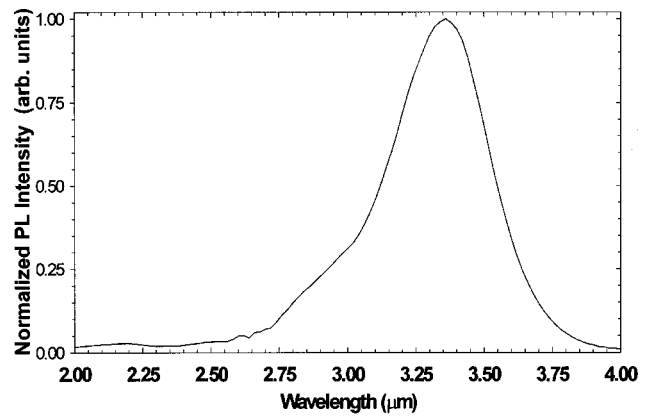


Fig. 7. Room temperature photoluminescence spectrum for a MQW sample with broken-gap wells and InAs/AlGaSb SL barriers. The photoluminescence is detected with a cooled (80 K) InSb photodiode, the output of which is fed into a lock-in amplifier. An 820 nm GaAs laser diode is used to provide $\sim 60 \text{ W/cm}^2$ of sample excitation intensity.

and intense x-ray superlattice and MQW fringes. Again, good agreement is obtained between the observed spectrum and one calculated for the structure using a dynamical x-ray model (Fig. 6). The measured MQW and superlattice fringe spacings indicate a 305 Å MQW period and 37.1 Å superlattice barrier period. Finally, the room temperature PL spectrum exhibited by this BGQW sample is shown in Fig. 7. The PL curve has a strong peak at the desired wavelength (3.4 μm), suggesting a high quality sample, with low defect densities.

The energy band structure in the BGQW is a significant improvement as compared to the previous laser active region designs. In particular, this structure offers a much greater degree of optimization of the final states in energy momen-

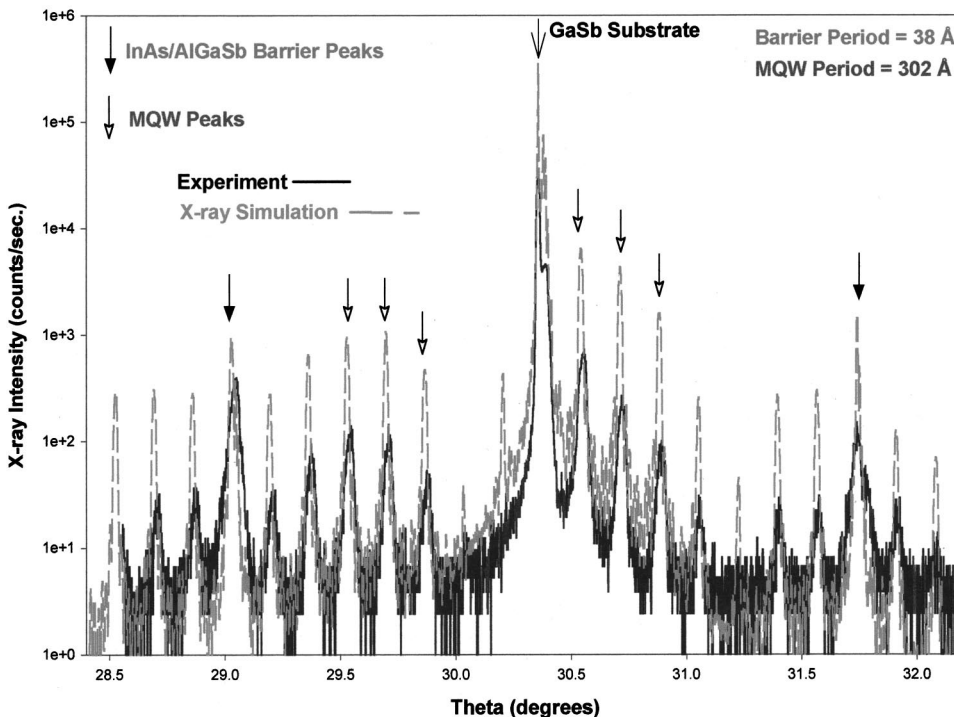


Fig. 6. X-ray spectrum for a MQW sample with InAs/AlAsSb/GaInSb BGQWs and InAs/AlGaSb superlattice barriers. The experimental data is depicted as the bold, solid curve and the dashed line represents the calculated spectrum. The closely spaced peaks (white arrows) are due to the MQW structure and the more intense, more widely spaced peaks (black arrows) are due to the InAs/AlGaSb superlattice barriers.

tum space in order to reduce ISBA. Pump/probe measurements performed on BGQW samples confirm the experimentally predicted reduction in AR. They yielded a 3 ns SRH lifetime and 0.94 ns Auger lifetime. Again, the Auger lifetime is measured at the calculated optimum carrier concentration ($n = 2.6 \times 10^{17} \text{ cm}^{-3}$) for room temperature, 3.4 μm laser operation (lower arrow in Fig. 3).⁶ Note that this Auger lifetime is factor of 2.7 longer than in the four-layer BGSL and 7.2 times longer than in the two-layer BGSL.

In summary, we have described the MBE growth of MWIR laser structures incorporating various broken-gap antimonide active regions. This work has culminated in the design and growth of a multiconstituent broken-gap quantum well structure that exhibits reduced nonradiative losses. Auger rates at carrier densities predicted to be optimal for lasing have been decreased by nearly an order of magnitude by appropriately tailoring the valence band structure.¹ Also, by employing antimony soaks in between the III–As and the III–Sb layers and by using the modulated shutter technique for the growth of the AlAsSb “quasi-ternary” compound, smooth, abrupt interfaces are obtained as evident from the x-ray diffraction data and the relatively long (3 ns) SRH lifetimes. However, further improvements in the material quality, and thus in the electrical and optical quality of the devices are possible through the use of the migration enhanced epitaxy technique at the critical interfaces.

ACKNOWLEDGMENTS

This research was supported in part by the United States Air Force, Air Force Materiel Command, Air Force Research

Laboratory, Kirtland AFB New Mexico 87117-5777 (Contract No. F29601-97-C-0041) and the National Science Foundation (Grants No. ECS 97-07799 and No. ECS 99-00486).

¹M. E. Flatté, J. T. Olesberg, S. A. Anson, T. F. Boggess, T. C. Hasenberg, R. H. Miles, and C. H. Grein, *Appl. Phys. Lett.* **70**, 3212 (1997).

²S. W. McCahon, S. A. Anson, D.-J. Jang, M. E. Flatté, T. F. Boggess, D. H. Chow, T. C. Hasenberg, and C. H. Grein, *Appl. Phys. Lett.* **68**, 2135 (1996).

³T. C. Hasenberg, D. H. Chow, A. R. Kost, R. H. Miles, and L. West, *Electron. Lett.* **31**, 275 (1995).

⁴T. C. Hasenberg, R. H. Miles, A. R. Kost, and L. West, *IEEE J. Quantum Electron.* **33**, 1403 (1997).

⁵D.-J. Jang, M. E. Flatté, C. H. Grein, J. T. Olesberg, T. C. Hasenberg, and T. F. Boggess, *Phys. Rev. B* **58**, 13 047 (1998).

⁶J. T. Olesberg, M. E. Flatté, B. J. Brown, C. H. Grein, T. C. Hasenberg, S. A. Anson, and T. F. Boggess, *Appl. Phys. Lett.* **74**, 188 (1999).

⁷M. E. Twigg, B. R. Bennett, P. M. Thibado, B. V. Shanabrook, and L. J. Whitman, *Optoelectronic Properties of Semiconductors and Superlattices* (Gordon and Breach Science, New York, 1997), Chap. 3.

⁸R. H. Miles, D. H. Chow, Y.-H. Zhang, P. D. Brewer, and R. G. Wilson, *Appl. Phys. Lett.* **66**, 1921 (1995).

⁹S. A. Anson, J. T. Olesberg, M. E. Flatté, T. C. Hasenberg, and T. F. Boggess, *J. Appl. Phys.* **86**, 713 (1999).

¹⁰M. E. Flatté, T. C. Hasenberg, J. T. Olesberg, S. A. Anson, Thomas F. Boggess, Chi Yan, and D. L. McDaniel, Jr., *Appl. Phys. Lett.* **71**, 3764 (1997).

¹¹Y.-H. Zhang and D. H. Chow, *Appl. Phys. Lett.* **65**, 25 (1994).

¹²J. T. Olesberg, T. C. Hasenberg, M. E. Flatté, and T. F. Boggess, *Appl. Phys. Lett.* (submitted).